sustainability

MDPI

Article

Sustainable Adsorbent Material Prepared by Soft Alkaline Activation of Spent Coffee Grounds: Characterisation and Adsorption Mechanism of Methylene Blue from Aqueous Solutions

Marco Cuccarese [1], Sergio Brutti [2], Angela De Bonis [3], Roberto Teghil [3], Francesco Di Capua [1], Ignazio Marcello Mancini [1], Salvatore Masi [1] and Donatella Caniani [1,*]

[1] School of Engineering, University of Basilicata, Viale dell'Ateneo Lucano n. 10, 85100 Potenza, Italy
[2] Department of Chemistry, University of Roma "La Sapienza", Piazzale Aldo Moro 5, 00185 Roma, Italy
[3] Department of Sciences, University of Basilicata, Viale dell'Ateneo Lucano n. 10, 85100 Potenza, Italy
* Correspondence: donatella.caniani@unibas.it

Abstract: Dyes are emerging as hazardous pollutants, which are the primary challenges for environmentalists. Dye removal from effluents is urgently needed. Adsorption technology has been widely employed in this context as an effective method for removing colours from the aqueous phase, and adsorption with the use of low-cost adsorbents has been shown to be more successful on a larger scale than other methods. In this study, spent coffee grounds (SCGs) were used as the precursor for the preparation of a low-cost activated carbon through the chemical activation with NaOH. The SCG sample was impregnated with NaOH and carbonised at 300 °C for three hours. Its morphological and physical-chemical properties were assessed using scanning electron microscopy (SEM), X-ray diffraction, and Raman spectroscopy analyses. The performance of the treated SCG as an adsorbent material for methylene blue (MB) was evaluated by analysing the effect of the initial pH ionic strength on the adsorption capacity and by evaluating the kinetics and the mechanisms of the process (using adsorption isotherms). The effect of the initial concentration (500 and 250 mg L^{-1}) of MB on the kinetics of the process and the impact of the initial pH (7.5 and 6) on the adsorption isotherm were evaluated. The obtained results show that the pseudo-second order model controls the process for both the investigated initial concentration and the adsorption capacity, which are 142.8 and 113.6 mg L^{-1}, respectively. The results indicate that the pH value influences the adsorption isotherm model that regulates the process. Specifically, this process is regulated by the Temkin's model with a pH of 7.5 and by the Langmuir's model with a pH of 6. The thermodynamics of the process were also determined. The results show that SCG, treated and carbonised by soft alkaline activation, is a promising low-cost adsorbent material as its performance is comparable to that of conventional active carbon materials.

Keywords: waste recycling; new adsorbent material; environmental sustainability; contaminated water remediation

Citation: Cuccarese, M.; Brutti, S.; De Bonis, A.; Teghil, R.; Di Capua, F.; Mancini, I.M.; Masi, S.; Caniani, D. Sustainable Adsorbent Material Prepared by Soft Alkaline Activation of Spent Coffee Grounds: Characterisation and Adsorption Mechanism of Methylene Blue from Aqueous Solutions. *Sustainability* **2023**, *15*, 2454. https://doi.org/10.3390/su15032454

Academic Editor: Iason Verginelli

Received: 29 November 2022
Revised: 19 January 2023
Accepted: 23 January 2023
Published: 30 January 2023

1. Introduction

Pollution in the ecosystem is frequently connected to population expansion and anthropogenic activities [1]. Water resource pollution is a highly controversial topic on a global scale since it has long-term, if not fatal, effects on living beings [2]. Dyes are complex-structured organic aromatic compounds that are soluble in water. A total of 700.000 tons of dye compounds are produced annually by the dye industry [3]. These industrial effluents, if dumped into the environment, can be dangerous because even a small amount of dye in water can cause colour, which is extremely hazardous to aquatic life. These dyes disrupt the photosynthesis of aquatic plants and block sunlight from penetrating

water, disrupting aquatic life in the process [4]. From all the dyes currently in use, 2% or so enter water streams through various paths and contaminate freshwater. It is challenging to remove dyes using chemical reagents because of their complex structures. Numerous sectors utilise a lot of dyes to colour their materials, including paper, plastic, rubber, leather, textile, cosmetics, food, and medicines [5]. The textile industry uses methylene blue (MB) extensively to colour paper, cotton, silk, and wool [5]. MB has a number of harmful effects on the human body, including serotonin poisoning, disorientation, precordial discomfort, and bladder irritation.

Traditional methods for removing colours from wastewater include physical, chemical, and biological processes. Precipitation, filtration, flocculation–coagulation, and reverse osmosis are examples of physical and chemical techniques.

Removing dyes via a chemical approach generates byproducts that contribute to pollution as a result of their disposal issues. The biological technique has limitations in terms of total colour removal. Adsorption has been identified as the most promising strategy for dye removal. Adsorption methods have the advantages of being economically practical, simple to handle, and of higher efficiency [5]. Activated carbons have found a wide range of uses and applications thanks to their porous structure, large availability, and neutral effect on the environment. Japan and the USA are the first consumers of these materials [6]. The increasing demand for activated carbons is caused by their growing applications in all industries in economically developed countries. Furthermore, activated carbons are the least expensive porous materials available. The production of activated carbons is mainly based on natural organic substrates, such as wood [7], sawdust [8], and waste products, such as fruit pits [9–12].

Adsorption using low-cost adsorbents has been discovered to be more effective on a wider scale than other approaches. Although commercially available activated carbons are excellent adsorbents, they raise the cost of colour removal. Despite their effectiveness in removing colours from industrial wastewater effluents, activated carbons have limitations, such as high capital costs, high energy consumption, and sorption–desorption cycles. Bio adsorbents derived from bacteria or fungus are potential environmentally friendly adsorbents for colour and heavy metal removal [13,14]. Nowadays, the most efficient adsorbents are activated carbons made from biowaste, agricultural waste, domestic and industrial waste, and minerals. These waste materials have disposal issues and have no considerable commercial value; hence, they are being investigated for the removal of dyes from industrial wastewater. Low-cost adsorbents are environmentally friendly, widespread, economical, and efficient for dye removal [15]. Many factors impact the properties of low-cost adsorbents. The precursor should be simple to obtain, inexpensive, and non-toxic. Recent studies have concentrated on natural solids that may remove contaminants from polluted water at a low cost. When comparing sorbents, price is an important consideration. A sorbent is termed "low cost" if it requires little processing, is abundant in nature, or is a byproduct of another industry. Many low-cost adsorbents, such as agricultural waste, natural materials, and bio-sorbents, have been used to remove colours. Their dye removal efficiency has been carefully examined. Waste-derived adsorbents have been selected as the most difficult field since they can clean wastewater while also reducing waste [16]. In an effort to produce more economical and effective adsorbents, several non-traditional low-cost adsorbents, such as zeolites, clay materials, agricultural wastes, siliceous material, and industrial waste products, have been proposed [17].

The morphological properties of activated carbons depend on the condition of the process of activation, such as the temperature of pyrolysis and the presence of the chemical activating agent. Normally, the surface area and the porosity obtained by using a simple pyrolysis are not enough to use activated carbons as an adsorbent material; hence, chemical activation is required [18–22]. Typical chemical activation is conducted with the use of phosphoric acid [22–24], but chemical activation with KOH by using pyrolysis conditions has been also reported [25–27]. A mechanism for alkaline activation was proposed in a study reported in the literature [27]. When the starting material is mixed with a KOH

solution, KOH or K^+ cations are intercalated in the carbon matrix. After dehydration, the carbon layers expand in the presence of K_2O derived from KOH (300 °C). As a consequence of carbon consumption, pores are formed in the carbon matrix. In Figure 1, a schematic representation of alkaline activation is reported.

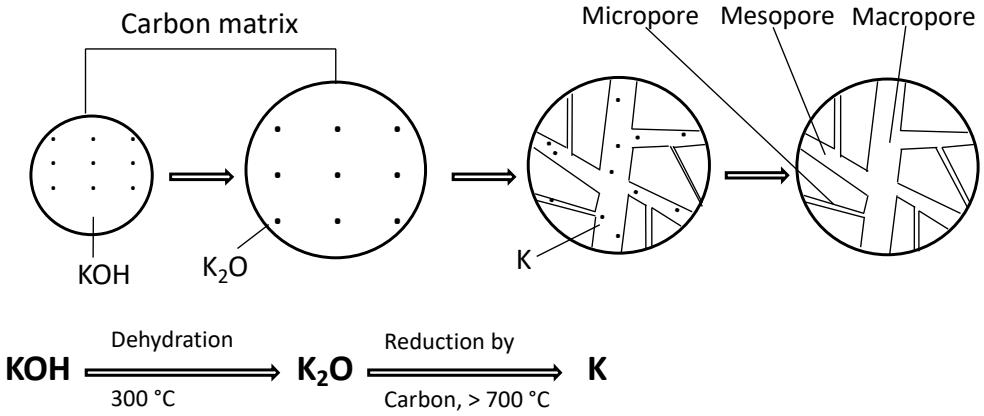

Figure 1. Schematic representation of alkaline activation.

When the activation temperature exceeds 700 °C, a considerable amount of metallic potassium is formed due to a reduction in K_2O by carbon at a high temperature. The effect of the use of KOH and NaOH as an alkaline medium on the morphological properties of activated carbons has been reported in the literature [28]. NaOH confers bigger surface areas and higher adsorption capacities to the non-pyrolysed precursors than KOH due to the higher expansion of carbon lamellae.

Coffee is one of the most traded agricultural commodities in the world. In 2017, the worldwide coffee industry processed around 9.6 million tonnes, according to the International Coffee Organisation (ICO). The most common coffee byproduct is spent coffee ground (SCG), which is a leftover from the coffee production. The vast majority of SCG is thrown away as waste. However, because of the inclusion of phenols, caffeine, and tannins, which are very hazardous to many biological processes, the release of SCG into the environment would pose a major concern [29]. SCG includes a variety of organic materials, such as lignin, cellulose, hemicellulose, and other polysaccharides that can be used to create value-added products. It has, therefore, been investigated for biodiesel synthesis as a source of sugars, as a compost, and as a raw material for antioxidant extraction. Only a few studies investigated its possible use as a precursor for activated carbon production [30], and none of them had the objective of using the obtained activated carbon to remove MB.

In an attempt to reduce this solid waste of SCG by producing useful material from it, this study aims to demonstrate the possibility of synthesising activated carbon from SCG by using a soft alkaline activation (300 °C and NaOH as alkaline medium) and its ability to remove an organic dye, i.e., MB. The adsorption capacity of this new material was studied through adsorption tests. The kinetics, isotherm adsorption, thermodynamics, pH, and ionic strength were also analysed in order to understand their possible influences on the process. Moreover, material characterisation studies were carried out.

2. Materials and Methods

2.1. Materials

SCG was obtained from the central cafeteria of the Basilicata University and then treated as reported in the Section 2. The initial pH of the solutions was adjusted by adding NaOH and HCl purchased from Carlo Erba (Carlo Erba, Rodano, Milano, Italy), as well as MB. The stock solution of MB was prepared at a concentration of 1000 mg/L. The reagents were of extra pure grade and were used without further purification. The solutions were prepared with distilled water.

2.2. Treatment of Spent Coffee Ground

A total of 13 g of SCG was washed with 1 L of the NaOH solution (1 M), and the two phases were stirred for 6 h to remove the soluble compounds present in the waste and to impregnate the SCG with NaOH. The washed solid phase, a very viscous slurry, was then carbonised in an oven overnight at 300 °C, resulting in a carbonaceous powder (11 g).

2.3. Material Characterisation

SEM images were obtained using a high-resolution field emission scanning electronic microscope (HR-FESEM, Auriga model, Zeiss.)

A LabRam micro-Raman spectrometer (HORIBA France SAS) with a He-Ne laser (λ = 632.8 nm), an edge filter, and an Olympus microscope with 10x, 50x, and 100x objectives was used for the analysis. A spectral resolution of about 5 cm^{-1} was obtained by a holographic grating with 600 grooves/mm. The spectra were acquired with an accumulation time of 60 s and a laser power of 20 mW.

The Fourier-transform infrared spectroscopy (FT-IR) spectrum was obtained in the range of 400–4000 cm^{-1} (4 cm^{-1} of resolution) by using a JASCO FT-IR 460 Plus spectrophotometer. The sample was measured in the form of KBr pellets.

2.4. Adsorption Test

The influence of pH, ionic strength, and initial concentration of MB on the adsorption capacity was evaluated. A total of 50 mL of the MB solution (500 mg/L) was mixed with 100 mg of the treated SCG in a 100 mL conical flask and stirred at 400 rpm for 30 min. After 30 min of contact time, the liquid phase was aspirated and analysed by using a UV-Vis spectrophotometer to determine the MB residue concentration. The adsorption capacity was measured by using Equations (1) and (2):

$$q = \frac{\text{mass of MB adsorbed (mg)}}{\text{mass of adsorbent (g)}} \quad (1)$$

$$q = (c_i - c_f)\,\frac{V}{m} \quad (2)$$

where c_I and c_f are the MB concentrations (mg L^{-1}) at the beginning and after each adsorption experiment, respectively; V is the initial solution volume (L); and m is the adsorbent weight (g).

The initial pH (1, 3, 4.5, 6, 7.5, and 9) of the MB solution was modified before the adsorption test by adding NaOH and HCl and monitoring the pH with a pHmeter (Orion 420A, ThermoFisher Scientific, Waltham, MA, USA). The initial ionic strength (0, 0.25, 0.5, 0.75, and 1 M) of the solution was modified by adding the required amount of NaCl. The initial concentrations of the MB tested were 500, 400, 250, 125, 100, and 25 mg L^{-1} at a pH of 7.5, and 1000, 500, 350, 250, 100, and 50 mg L^{-1} at a pH of 6. All tests were performed in duplicate.

2.5. Kinetic Studies

In order to evaluate the kinetics of the adsorption process and the relationship between the contact time and the adsorption capacity, the same experimental setup described above was used but at different contact times (5, 10, 15, 30, 40, and 60 min). Therefore, 50 mL of the MB solution (500 and 250 mg/L) was mixed with 100 mg of the treated SCG and stirred at 400 rpm for different contact times at a pH of 7.5 (optimal pH). Two different concentrations of MB were used to verify the influence of the initial concentration on the kinetics of the process. The adsorption capacity was evaluated and reported versus the contact time. All tests were repeated three times to obtain the mean value.

The experimental data were fitted to five kinetic mathematical models, i.e., pseudo-first order, pseudo-second order, intraparticle diffusion, Elovich, and liquid film diffusion models, in order to interpret the mechanism of adsorption of the MB on the treated

SCG and evaluate the slowest step of the process. Table 1 shows the linear form of the model equations.

Table 1. Overview of the kinetic models used in this study.

Model	Equation	References
Pseudo-first order	$\log(q_e - q_t) = \log(q_e) - k_1 t$	[28]
Pseudo-second order	$\frac{t}{q_t} = \frac{1}{k_2 q_e^2} + \frac{t}{q_e}$	[28]
Elovich	$q_t = \frac{1}{\beta}\ln(\alpha\beta) + \frac{1}{\beta}\ln(t)$	[29]
Liquid film diffusion	$\ln\left(1 - \frac{q_t}{q_e}\right) = -k_{fd} t$	[30]
Intraparticle diffusion	$q_t = k_{dif} t^{1/2} + C$	[30]

Table 1 presents an overview of the kinetic models used in this study. q_e is the equilibrium adsorption capacity (mg g^{-1}); q_t is the adsorption capacity at time t (mg g^{-1}); k_1 is the rate constant of the pseudo-first order (min^{-1}); k_2 is the rate constant of the pseudo-second order (g mg^{-1} min^{-1}); α and β are the initial adsorption rate of the Elovich equation and the desorption constant related to the extent of surface coverage and activation energy constant for chemisorption (mg g^{-1} min^{-1}) (g mg^{-1}); k_{fd} is the liquid film rate diffusion constant (min^{-1}); and k_{dif} is the rate constant of intraparticle diffusion (mg g^{-1} $min^{-1/2}$).

The surface area covered by the MB (S_{MB}) was calculated by using the following equation [31]:

$$S_{MB} = q_e \cdot A_M \cdot 6.02 \times 10^{23} / M_{MB}$$

where q_e is the adsorption capacity (g g^{-1}); A_M is the molecular surface of the MB (1.3 nm^2); and M_{MB} is the molecular weight of the MB.

2.6. Adsorption Isotherm

The adsorption isotherm of the MB on the treated SCG was used to further investigate the adsorption mechanism. The effect of pH on the adsorption isotherm was studied in particular. Therefore, 50 mL of the MB solution at different initial concentrations (1000, 500, 350, 250, 100, and 50 mg/L) at a pH of 6 and 50 mL of the MB solution at different initial concentrations (500, 400, 250, 125, 100, and 25 mg/L) at a pH of 7.5 were prepared. pH 6 and 7.5 were chosen because they are close to neutrality and require no additional steps to reintroduce water into the environment after treatment. Each solution was mixed in a 100 mL conical flask with 100 mg of the treated SCG and stirred at 400 rpm for 30 min. Afterwards, the liquid phase was aspirated, the residual concentration of the MB was determined by a UV-Vis spectrophotometric analysis, and the adsorption capacity was calculated. All tests were performed in duplicate. The data obtained were fitted with the Langmuir [31], Freundlich [32,33], Temkin [34], and Dubinin–Radushkevich [35] isotherm models.

The Langmuir model assumes a monolayer adsorption on a surface that contains a finite number of identical sites; therefore, in this case, the adsorption is uniform. The linear form of the equation is reported in Equation (3):

$$\frac{C_e}{q_e} = \frac{1}{K_L\, q_m} + C_e / q_m \quad (3)$$

where C_e is the adsorbate concentration at equilibrium in the liquid phase (mg L^{-1}); q_e is the adsorption capacity at equilibrium (mg g^{-1}); K_L (L mg^{-1}) is a constant associated with the free energy of the process; and q_m (mg g^{-1}) is the maximum adsorption capacity (mg g^{-1}).

The Freundlich model assumes a multilayer adsorption, with a set of nearby sites on the adsorbent's surface. The linear form of the equation is given in Equation (4):

$$\ln q_e = \ln K_f + \frac{1}{n_F} ln C_e \quad (4)$$

where K_f indicates the adsorption capacity ((mg g^{-1}) (L $mg^{-1})^{1/n}$), and $\frac{1}{n_F}$ defines the adsorption intensity.

The Temkin model assumes that the adsorbent–adsorbate interaction causes a linear decrease in the adsorption heat of all the molecules in the layer. Moreover, it supposes that the adsorption is characterised by a uniform distribution of the binding energies up to a maximum binding energy. The linear form of the equation is reported in Equation (5):

$$q_e = B_1 \ln A + B_1 \ln C_e \quad (5)$$

where A is the equilibrium binding constant (L g^{-1}) and B_1 is related to the heat of adsorption (J mol^{-1}).

The Dubinin–Radushkevich model assumes that a heterogeneous surface with a steric hindrance between the adsorbed and incoming particles is involved in the adsorption process. The linear form of the equation is presented in Equation (6):

$$\ln(q_e) = \ln(q_s) - \beta\varepsilon^2 \quad (6)$$

$$\varepsilon = RTln\left(1 + \frac{1}{C_e}\right) \quad (7)$$

$$E = \frac{1}{-\sqrt{2\beta}} \quad (8)$$

where β is the Dubinin–Radushkevich constant (mol^2 J^{-2}); E is related to free energy (kJ mol^{-1}); ε is the Polanyi potential; and q_s is the adsorption capacity (mg g^{-1}).

2.7. Thermodynamic Study

The driving force, the free energy of the process, and the minimum temperature that ensures the spontaneity of the process can be determined by evaluating the thermodynamics of the process. Therefore, 50 mL of the MB solution (500 mg/L) at a pH of 7.5 was mixed with 100 mg of the treated SCG and stirred at 400 rpm for 30 min. The adsorption capacity was evaluated at different temperatures (293, 313, and 323 K), which were controlled with a magnetic stirring system equipped with a heat control system. All tests were performed in duplicate. The following relationships (Equations (9) and (10)) were used to evaluate the thermodynamics of the process [32]:

$$\Delta G^\circ = -RT\, ln\frac{q_e}{C_e} \quad (9)$$

$$\Delta G^\circ = \Delta H^\circ - T\Delta S^\circ \quad (10)$$

where ΔG° is the standard free energy; q_e is the adsorption capacity; C_e is the concentration of the adsorbate at equilibrium; ΔH° is the standard enthalpy; T is the temperature; and ΔS° is the standard entropy.

The following Equation (11) can be obtained from Equations (9) and (10):

$$ln\frac{q_e}{C_e} = -\Delta H^\circ/RT + \Delta S^\circ/R \quad (11)$$

To understand the driving force of the process and to calculate the enthalpy and the entropy of the process, $ln\frac{q_e}{C_e}$ versus 1/T was plotted. The intercept and the angular coefficient of the obtained graph are related to the enthalpy and the entropy of the process.

3. Results and Discussions

3.1. Material Characterisation

The textural properties of the treated SCG were evaluated by performing a SEM analysis. Figure 2 illustrates the SEM images acquired by using different magnifications.

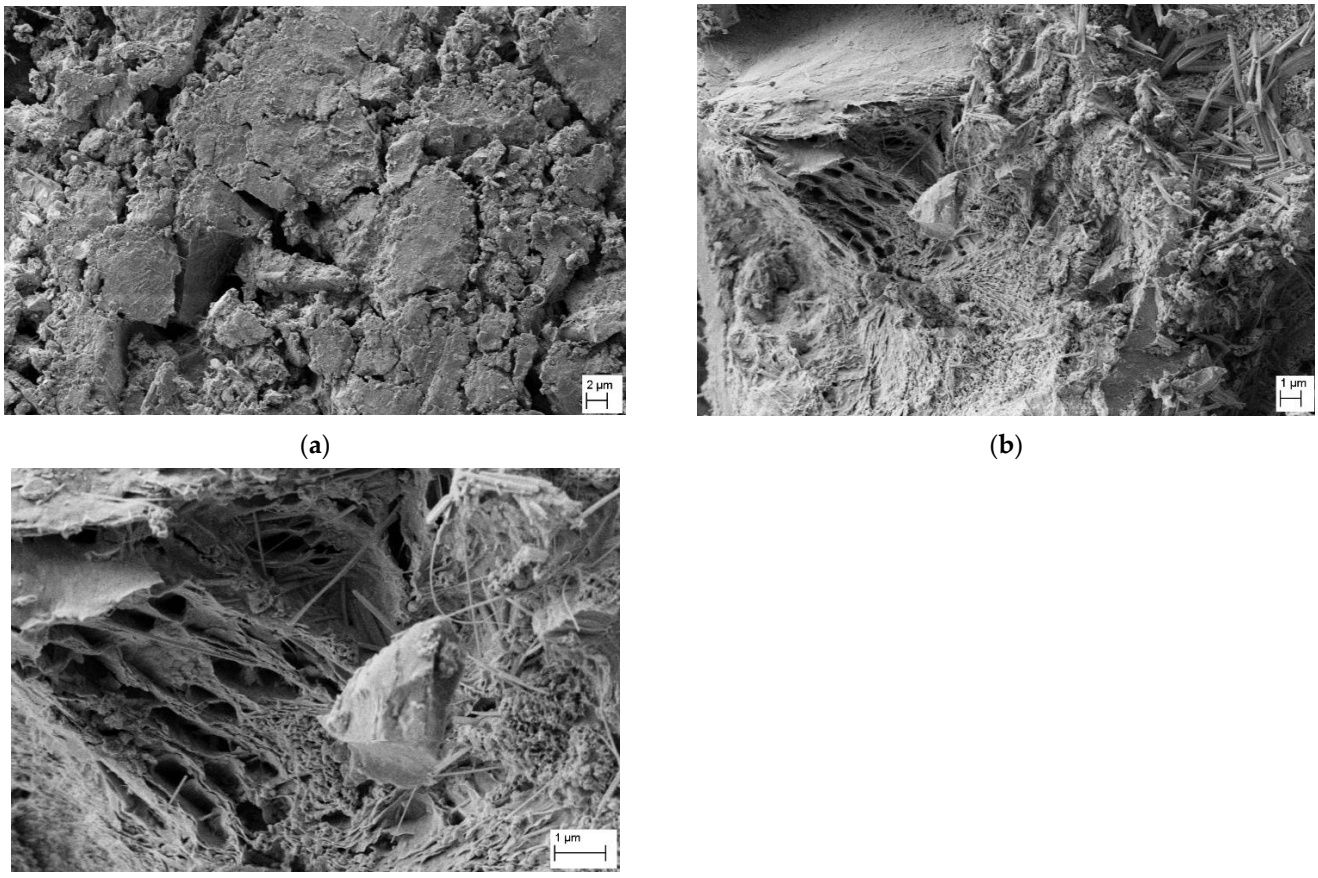

(**a**) (**b**)

(**c**)

Figure 2. SEM images acquired with different magnifications ((**a**): 5000 X, (**b**): 10000 X, and (**c**): 25000 X).

The SEM images reveal the roughly heterogeneous surface of the treated SCG (Figure 2). The residues of the activating agent are probably present on the surface of the coffee. The formation of pores can be seen in the higher-magnification images. This confirms that the temperature used (300 °C) is involved in the dehydration of the water that impregnates the SCG and a partial reduction of sodium oxides by carbon. The typical honeycomb structure obtained with pyrolysis at about 700 °C reported in the literature [36,37] can be observed, even if it is not extended to the entire surface of the material. As demonstrated subsequently, the porosity obtained is enough to obtain an adsorption capacity comparable with materials pyrolysed at a higher temperature than that applied in this study. In Figure 3, the Raman spectrum is shown, and the broad peak at about 1500 cm^{-1} confirms the carbonaceous amorphic structure of the treated SCG.

In Figure 4, the FT-IR spectrum in the range of 400–4000 cm^{-1} obtained for the treated (TGC) and non-treated coffee ground (GC) are reported.

The broad peak at about 3400 cm^{-1} is typically attributed to hydroxyl groups, and it seems to be more intense in the non-treated SCG, while the band located at about 2900 cm^{-1} corresponds to the C-H stretching vibrations, and it is more intense in the non-treated SCG. The band at about 2300 cm^{-1} can be attributed to the stretching of the triple bond C-C and is present only in the treated SCG. The band at about 1600–1400 cm^{-1} can be associated with the stretching of the double bond C-C of alkene compounds, the C-H bending, and the bending of the N-H bond. This band is present in the treated SCG, while the peak at

about 1400 cm^{-1} is lower in the non-treated SCG; the peak at about 1600 cm^{-1} is shifted to about 1700 cm^{-1} in the non-treated SCG, and it could be associated with the stretching of the C=O bond. The band at 1000 cm^{-1} associated with the alcohol groups is present in the non-treated SCG. The band in the range of 780–880 cm^{-1} can be associated with the C-H aromatic bond, and it is present only in the treated SCG.

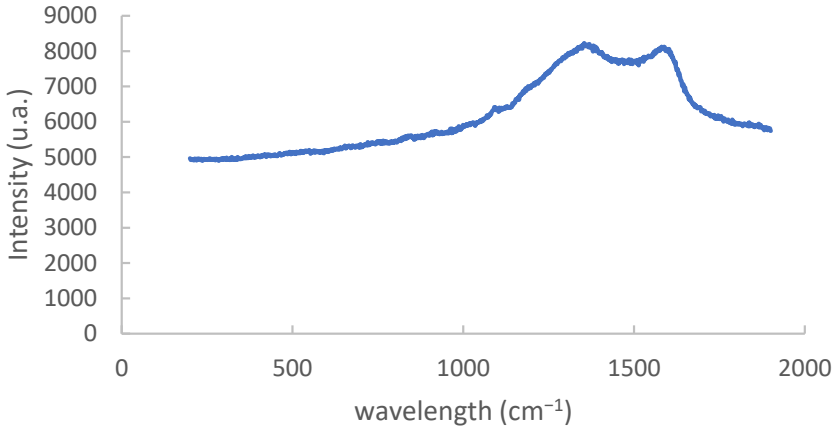

Figure 3. Raman spectrum of treated coffee ground.

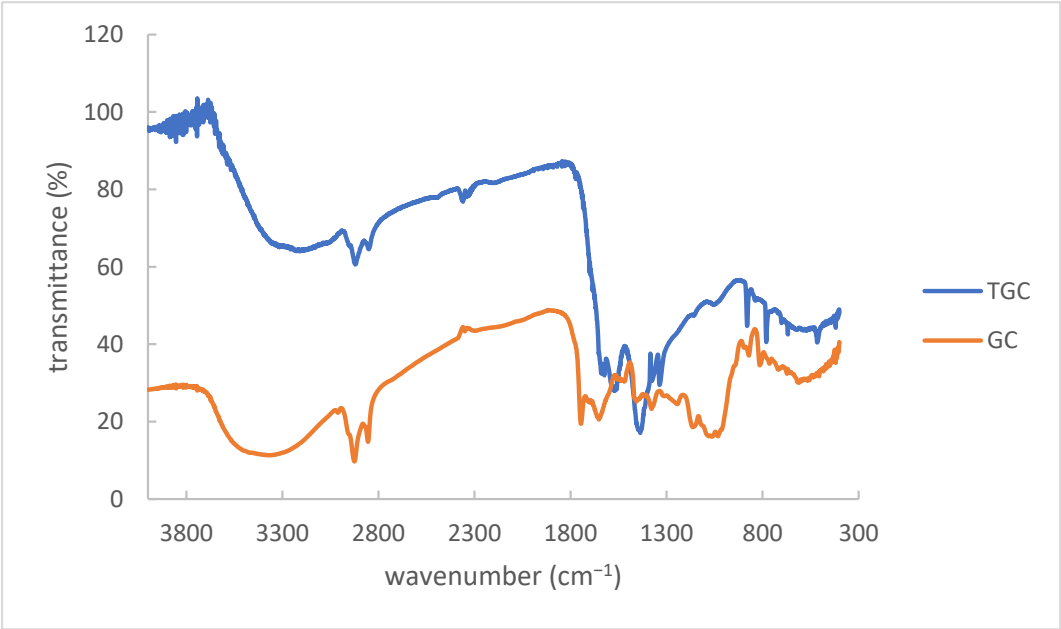

Figure 4. FT-IR spectrum of the treated coffee ground (TGC) and the coffee ground without treatment (GC).

3.2. pH Influence

In Figure 5, the variation in the adsorption capacity of the treated SCG for the MB at different values of pH is reported. The error bars representing the standard deviations are also shown.

The decrease in the pH involves a decrease in the adsorption capacity due to the protonation of the adsorbent's functional groups and/or surface (MB is positively charged) and a decrease in the electrostatic interaction between the adsorbate and the adsorbent [38–41]. In contrast, the large amount of OH^- at a high pH negatively influences the adsorption capacity due the possible neutralization of MB and a decrease in the electrostatic interaction. Therefore, an optimal pH value is obtained when these detrimental pH effects are minimised.

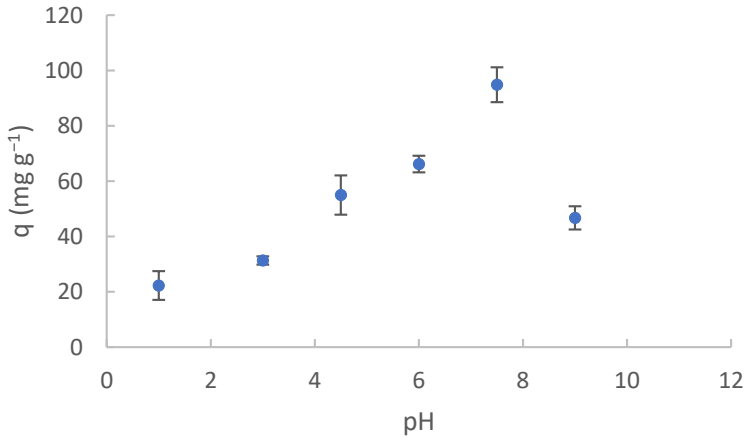

Figure 5. Effect of pH on MB removal by the treated SCG. C_o = 500 mg L^{-1}, contact time = 30 min, solution volume = 50 mL, mass of adsorbent = 100 mg, and stirring speed = 400 rpm.

3.3. Effect of Ionic Strength

Figure 6 shows the influence of ionic strength on the adsorption capacity of the treated SCG towards the MB. The profile of the average adsorption capacities obtained at different ionic strengths is outlined with the standard deviations.

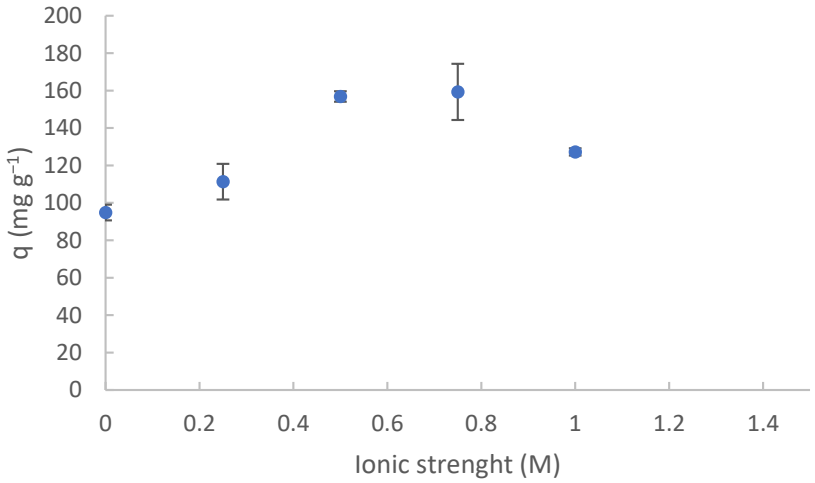

Figure 6. Effect of ionic strength on MB removal by the treated SCG. C_o = 500 mg L^{-1}, contact time = 30 min, solution volume = 50 mL, mass of adsorbent = 100 mg, stirring speed = 400 rpm, and Ph = 7.5.

The maximum adsorption capacity (159.3 mg g^{-1}) is obtained at 0.75 M. The increase in ionic strength is associated with an initially increased adsorption capacity, probably due to an increase in the solubility of the MB caused by the salt effect. The same increase in adsorption capacity with an increase in ionic strength is reported in the literature [42], even if the ionic strength used in this study is higher. At ionic strengths greater than 0.75 M, the adsorption capacity decreases, most likely due to a hindering effect caused by the high concentration of negatively charged sodium ions and/or the competition between the MB and positively charged ions added to the solution [43].

3.4. Kinetic Studies

The influence of the contact time for different values of the initial concentration of MB on the adsorption capacity was evaluated, and the results are reported in Figure 7. The error bars indicating the standard deviations are also shown.

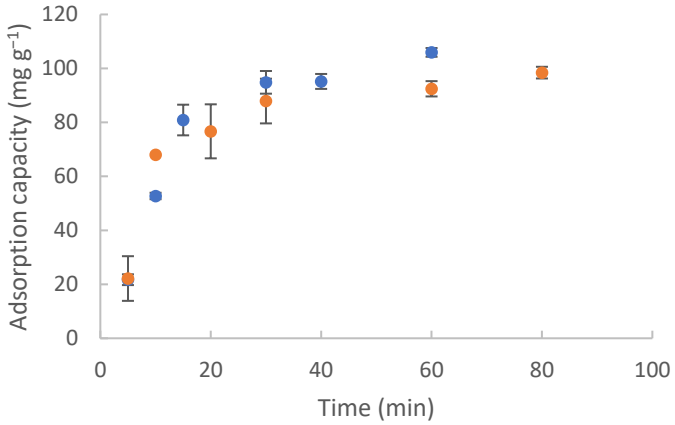

Figure 7. Effect of contact time on MB removal by the treated SCG. C_o = 500 mg L^{-1} (blue circle), 250 mg L^{-1} (orange circle), contact time = 30 min, solution volume = 50 mL, mass of adsorbent = 100 mg, and stirring speed = 400 rpm, pH = 7.5.

An increase in the adsorption capacity with increasing contact time can be observed in the first 30 min of the treatment, then a plateau is reached. Therefore, the optimum contact time can be fixed at 30 min, which corresponds to the maximum adsorption capacity of about 100 mg g^{-1}. This trend is typical of that described in the literature, and it is interesting to note that the initial concentration of the MB has no significant influence on the kinetics of the process. Table 2 summarises the kinetic parameters and the coefficient of correlation calculated by fitting the experimental data with the already cited kinetic models.

Table 2. Fitting of the experimental data with existing kinetics models.

		500 mg L^{-1}		**250 mg L^{-1}**
Model	**R^2**	**Parameters**	**R^2**	**Parameters**
Pseudo-first order	0.861	$K_1 = 1.15 \times 10^{-1}$ min^{-1} $q_e \approx 10^5$ mg g^{-1}	0.912	$K_1 = 5.46 \times 10^{-2}$ min^{-1} $q_e \approx 10^4$mg g^{-1}
Pseudo-second order	0.932	$q_e = 142.8$ mg g^{-1} $k_2 = 3.7 \times 10^{-4}$ g mg^{-1} min^{-1}	0.973	$q_e = 113.64$ mg g^{-1} $k_2 = 7.3 \times 10^{-4}$ g mg^{-1} min^{-1}
Elovich	0.829	$\beta = 3 \times 10^{-2}$ mg g^{-1} min^{-1} $\alpha = 16.7$ g mg^{-1}	0.715	$\beta = 4.1 \times 10^{-2}$ mg g^{-1} min^{-1} $\alpha = 22.7$ g mg^{-1}
Intraparticle diffusion	0.929	$K_{dif} = 14.04$ mg g^{-1} $min^{-1/2}$ C = 7.76	0.852	$K_{dif} = 9.02$ mg g^{-1} $min^{-1/2}$ C = 26.10
Liquid film diffusion	0.861	$K_{fd} = 1.15 \times 10^{-1}$ min^{-1}	0.912	$K_{fd} = 5.46 \times 10^{-2}$ min^{-1}

By analysing the results of the fit of the experimental data with the kinetics models, it is possible to note that the pseudo-second order model is the best fit for the experimental data for the MB concentrations of 500 and 250 mg L^{-1}, which indicates that the concentration does not affect the kinetics of the process and a chemisorption is observed. For the concentration of 250 mg L^{-1} of MB, the fit with the pseudo-second order model gives a value of 113.6 mg g^{-1} for the adsorption capacity (about 100 mg g^{-1} based on the experimental data). For a concentration of 500 mg L^{-1}, the intraparticle diffusion model results in a higher R^2 coefficient than the liquid film diffusion model, and the value obtained for R^2 allows us to say that intraparticle diffusion is the limiting step for adsorption, while at 250 mg L^{-1}, the limiting step is liquid film diffusion. The value of 142.8 mg g^{-1} for q_e obtained from the pseudo-second order model at the initial MB concentration of 500 mg L^{-1} is higher than that at 250 mg L^{-1} (113.6 mg g^{-1}), which is very close to the experimental data (about 100 mg g^{-1}) and indicates that the best fit is obtained for the data collected at the initial concentration of 250 mg L^{-1}. The surface area covered by the MB

is 311.39 m^2 g^{-1} at C_0 = 250 mg L^{-1} and 393.50 m^2 g^{-1} at C_0 = 500 mg L^{-1}. The value of the adsorption capacity obtained is higher or comparable with other values reported in the literature for pyrolysed or activated SCGs [44,45] or untreated coffee residues [38,44,46]. A comparison of the absorption capacities obtained in this study and those obtained with other activated carbons derived from different or the same biosources is reported in Table 3. It is important to note that the activation method for SCG developed in this study is rather effective, as it obtains adsorption efficiency values that are comparable to or higher than the literature values, but with much lower activation temperatures.

Table 3. Comparison of the adsorption capacity for different adsorbent materials derived from different bioresources.

Material	Adsorption Capacity (mg g^{-1})	References
SCG activated by alkaline medium at 300 °C	113.64 (C_0 = 250 mg L^{-1}) 142.80 (C_0 = 500 mg L^{-1})	This work
SCG activated by microwave heating (alkaline activation)	99.43	[47]
Coffee residues	6.76	[45]
SCG pyrolysed at 850 °C	129.90	[46]
Coffee residues	4.68	[39]
SCG activated by phosphoric acid at 450 °C	367.00	[48]
Pine fruit shell	529.00	[49]
Black stone cherries	321.75	[11]
Walnut shell	315.00	[50]
Oil palm shell	243.90	[51]
Hazelnut husks	204.00	[52]
Plant leaf powder	61.22	[53]
Wood apple rind	40.00	[54]
Cherry stones	276.00	[55]
Rice husks	441.52	[56]

3.5. Adsorption Isotherm

The adsorption isotherms obtained at the initial pH values of 6 and 7.5 are reported in Figure 8. The standard deviation of each data point is also reported.

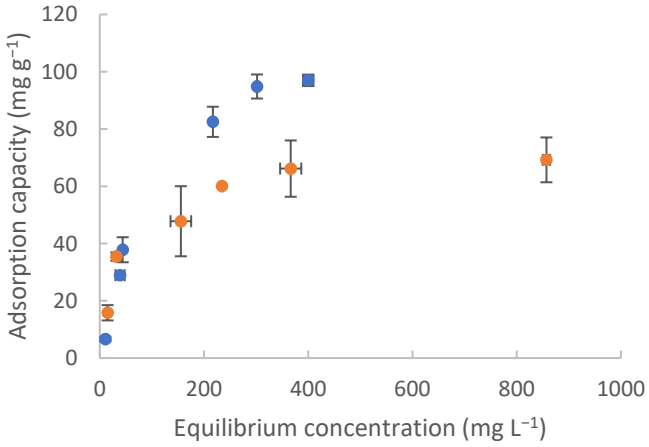

Figure 8. Isotherm adsorption at different values of pH (6 orange circle and 7.5 blue circle). C_0 = 500, 400, 250, 125, 100, and 25 mg L^{-1} for a pH of 7.5, and C_0 = 1000, 500, 350, 250, 100, and 50 mg L^{-1} for a pH of 6, with 100 mg of adsorbent material, stirring speed = 400 rpm, and contact time = 30 min.

As expected, the adsorption capacity increases with an increase in the equilibrium concentration until it reaches a plateau at 300 mg L^{-1} at a pH of 7.5 with a q_{max} of about 100 mg g^{-1} and at 400 mg L^{-1} at a pH of 6 with a q_{max} of about 60 mg g^{-1}. In Table 4, the equations of the linear regression and R^2 coefficient of the experimental data fitted with each model are reported.

Table 4. Fit of the adsorption isotherm data by using the Langmuir, Freundlich, Temkin, and Dubinin–Radushkevich models.

	pH 7.5		pH 6	
Model	**R^2**	**Equation**	**R^2**	**Equation**
Langmuir	0.922	$y = 6.5 \times 10^{-3}x + 1.18$	0.983	$y = 1.3 \times 10^{-2}x + 0.73$
Freundlich	0.934	$y = 0.75x + 0.42$	0.896	$y = 0.39x + 1.89$
Temkin	0.983	$y = 26.98x - 62.68$	0.957	$y = 14.42x - 20.08$
Dubinin–Radushkevich	0.841	$y = -5 \times 10^{-5}x + 4.09$	0.938	$y = -5 \times 10^{-5}x + 4.02$

By varying the pH, a change in the mechanism of interaction happens. In particular, at a pH of 7.5, the model that best fits the experimental data is the Temkin model, while at a pH of 6, the Langmuir model is the best fit for the experimental data. Therefore, at a pH of 7.5, the adsorbate interacts with a heterogeneous surface, and a multilayer of adsorbate on the adsorbent may be present. On the other hand, the increase in the H^+ concentration at a pH of 6.5 causes the adsorption of just one layer of MB due to the reduction in the electrostatic interaction, and the surface could become more homogeneous as H^+ is adsorbed on it. The q_{max} values reported previously support these hypotheses (100 mg g^{-1} at a pH of 7.5 vs. 60 mg g^{-1} at a pH of 6). The Langmuir constant is calculated to be 1.8×10^{-2} L mg^{-1}, and the q_{max} is calculated to be 76.92 mg g^{-1}. The value of the separation factor is between zero and one for each value of the initial concentration; therefore, the process is favorable. The value of the equilibrium binding constant calculated by the Temkin model is 0.099 L g^{-1}, and the value of B_1 (related to the heat of adsorption) is 26.98 J mol^{-1}. The adsorption capacity evaluated by isothermal adsorption is comparable with the values reported in the literature [38,43,45].

3.6. Influence of Initial Concentration

Figure 9 shows the influence of different initial concentrations of the MB on the adsorption capacity at different pH values.

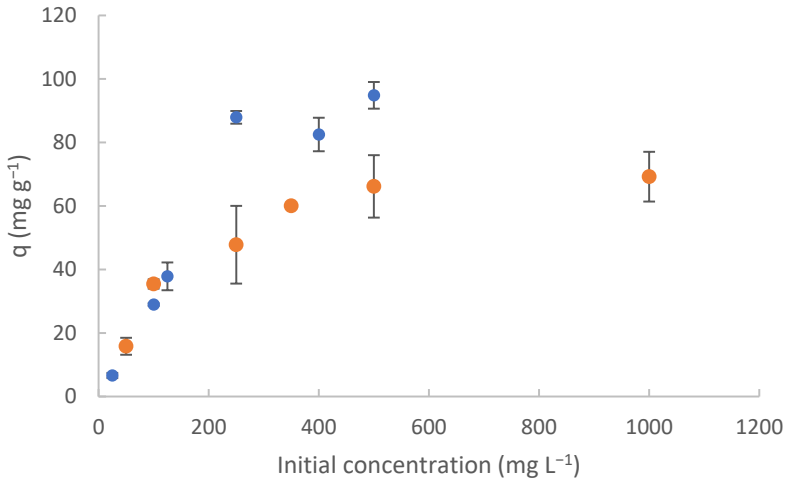

Figure 9. Adsorption capacity at different initial concentrations of MB. C_0 = 500, 400, 250, 125, 100, and 25 mg L^{-1} at a pH of 7.5 (blue circle), and C_0 = 1000, 500, 350, 250, 100, and 50 mg L^{-1} at a pH of 6 (orange circle), with 100 mg of adsorbent material, stirring speed = 400 rpm, and contact time = 30 min.

An initial rapid increase in adsorption capacity is observed by increasing the initial concentration of MB at both pH values. A plateau is reached at an initial MB concentration of about 250 mg L^{-1} at a pH of 7.5 and about 350 mg L^{-1} at a pH of 6. The different minimum initial concentration required to reach the plateau is associated with a different adsorption capacity of the material at the different pH conditions, and it could be linked to the considerations made above on the formation of a multilayer of MB at a pH of 7.5, which happens differently than what happens at a pH of 6.

3.7. Thermodynamic Studies

The thermodynamics of the adsorption process of MB on the treated SCG were evaluated through the estimation of several parameters, including the standard enthalpy, the standard entropy, the standard free energy, and the minimum temperature of spontaneity. The values obtained in this study are reported in Table 5.

Table 5. Thermodynamic parameters of the adsorption process of MB on the treated SCG.

ΔH (kJ mol^{-1})	ΔS (J mol^{-1} K^{-1})	ΔG° (kJ mol^{-1})	T_{min} (°C)
1.28	7.10	−0.84	−83

The process is driven by an increase in the entropy caused by an increase in randomness at the liquid/solid interface. The results show that the process is endothermic, so the increase in temperature promotes the process in terms of the equilibrium position and velocity. The value of free energy demonstrates that physiochemical adsorption occurs. The value of the free energy obtained and the physical adsorption observed are comparable to the literature data [56,57]. Moreover, in Table 6, it is possible to note the perfect correlation between the experimental and theoretical data of the free energy and equilibrium constant ΔG°.

Table 6. Equilibrium constant and free energy values obtained from the experimental and theoretical data. The experimental data are obtained for an adsorption test with 500 mg L^{-1} of MB solution, 100 mg of adsorbent material, pH of 7.5, stirring speed = 400 rpm, and contact time = 30 min.

Temperature (K)	$\frac{q_e}{C_e}$ Experimental (mg L^{-1})	$\frac{q_e}{C_e}$ Theoretical (mg L^{-1})	ΔG° Experimental (kJ mol^{-1})	ΔG° Theoretical (kJ mol^{-1})
293	1.39	1.39	−0.80	−0.80
313	1.43	1.45	−0.94	−0.94
323	1.46	1.46	−1.02	−1.01

4. Conclusions

This study shows that SCG treated and carbonised by soft alkaline activation is a promising adsorbent material that can be useful for environmental safeguards. The results show that the performance of this activated carbon is comparable to that of other active carbons derived from other biosources and/or activated with different processes. There are no special or difficult conditions required to remove MB from an aqueous solution by adsorption because the very low minimum temperature of spontaneity in the process ensures feasibility even in the winter if the process is carried out outdoors. The kinetics, isothermal adsorption, thermodynamics, pH, and ionic strength were shown to influence the process. The neutral pH required for the treatment allows the reintroduction of the treated water into the natural cycle of water without further treatment.

Further studies can be conducted to examine the possibility of removing other pollutants and determine SCG's related adsorption capacity. Therefore, this study shows a practical example of upcycling a waste product of the agri-food industry into a resource, which is in line with the targets of the new European Green Deal proposed by the European Commission.

Author Contributions: Conceptualisation, M.C., S.B., A.D.B., R.T., I.M.M., S.M. and D.C.; Methodology, M.C., S.B., A.D.B., R.T., I.M.M., S.M., F.D.C. and D.C.; Validation, M.C., S.B., A.D.B., R.T., I.M.M., S.M., F.D.C. and D.C.; Formal analysis, M.C., S.B., A.D.B., R.T., F.D.C., I.M.M. and S.M.; Investigation, M.C., S.B., A.D.B., R.T., S.M. and D.C.; Resources, S.M. and D.C.; Data curation, M.C., S.B., A.D.B. and D.C.; Writing—original draft, M.C., S.B., A.D.B., R.T., I.M.M., S.M. and D.C.; Writing—review and editing, F.D.C. and D.C.; Visualisation, F.D.C., I.M.M., S.M. and D.C.; Supervision, R.T., I.M.M., S.M. and D.C.; Project administration, D.C. and S.M. All authors have read and agreed to the published version of the manuscript.

Funding: This research received no external funding.

Institutional Review Board Statement: Not applicable.

Informed Consent Statement: Not applicable.

Data Availability Statement: The data presented in this study are available on request from the corresponding author.

Conflicts of Interest: The authors declare no conflict of interest.

References

1. Hokkanen, S.; Bhatnagar, A.; Sillanpaa, M. A review on modification methods to cellulose-based adsorbents to improve adsorption capacity. *Water Res.* **2016**, *91*, 156–173. [CrossRef] [PubMed]
2. Inamuddin. Xanthan gum/titanium dioxide nanocomposite for photocatalytic degradation of methyl orange dye. *Int. J. Biol. Macromol.* **2018**, *121*, 1046–1053. [CrossRef] [PubMed]
3. Katheresan, V.; Kansedo, J.; Lau, S.Y. Efficiency of various recent wastewater dye removal methods: A review. *J. Environ. Chem. Eng.* **2018**, *6*, 4676–4697. [CrossRef]
4. Adegoke, K.; Bello, O. Dye sequestration using agricultural wastes as adsorbents. *Water Resour. Ind.* **2015**, *12*, 8–24. [CrossRef]
5. Shelke, B.N.; Jopale, M.K.; Kategaonkar, A.H. Exploration of biomass waste as low cost adsorbents for removal of methylene blue dye: A review. *J. Indian Chem. Soc.* **2022**, *99*, 100530. [CrossRef]
6. Bansal, R.; Goyal, M. *Activated Carbon Adsorption*; Taylor & Francis Group: Boca Raton, FL, USA, 2005.
7. Wang, T.; Tan, S.; Liang, C. Preparation and characterization of activated carbon from wood via microwave-induced $ZnCl_2$ activation. *Carbon* **2009**, *47*, 1867–1885. [CrossRef]
8. Pietrzak, R. Sawdust pellets from coniferous species as adsorbent for NO_2 removal. *Bioresour. Technol.* **2010**, *101*, 907–913. [CrossRef]
9. Chen, X.; Jeyaseelan, S.; Graham, N. Physical and chemical properties studies of activated carbon made from sewage sludge. *Waste Manag.* **2002**, *22*, 755–760. [CrossRef]
10. Dilek, A. Production and characterization of activated carbon from sour cherry stones by zinc chloride. *Fuel* **2014**, *115*, 804–811.
11. Arana, J.R.; Mazzocco, R. Adsorption studies of methylene blue and phenol onto black stone cherries prepared by chemical activation. *J. Hazard. Mater.* **2010**, *180*, 656–661. [CrossRef]
12. Tennison, S.R. Phenolic-resin derived activated carbons. *Appl. Catal. A Gen.* **1998**, *173*, 289–311. [CrossRef]
13. Vital, R.K.; Saibaba, K.V.N.; Shaik, K.B. Dye Removal by Adsorption: A Review. *J. Bioremediation Biodegrad.* **2016**, *7*, 371.
14. Staroń, P.; Chwastowski, J. Raphia-Microorganism Composite Biosorbent for Lead Ion Removal from Aqueous Solutions. *Materials* **2021**, *14*, 7482. [CrossRef] [PubMed]
15. Teng, H.; Wang, S. Preparation of porous carbons from phenol-formaldehyde resins with chemical and physical activation. *Carbon* **2000**, *38*, 817–824. [CrossRef]
16. Hamad, H.N.; Idrus, S. Recent Developments in the Application of Bio-Waste-Derived Adsorbents for the Removal of Methylene Blue from Wastewater: A Review. *Polymers* **2022**, *14*, 783. [CrossRef] [PubMed]
17. Rauf, M.A.; Shehadeh, I.; Ahmed, A.; Al-zamly, A. Removal of Methylene Blue from Aqueous Solution by Using Gypsum as a Low Cost Adsorbent. *World Acad. Sci. Eng. Technol.* **2009**, *55*, 608–613.
18. Ariyadejwanich, P.; Tanthapanichakoon, W.; Nakagawa, K.; Mukai, S.; Tamon, H. Preparation and characterization of mesoporous activated carbon from waste tires. *Carbon* **2003**, *41*, 157–164. [CrossRef]
19. Lee, W.; Reucroft, P. Vapor adsorption on coal- and wood-based chemically activated carbons (II) adsorption of organic vapors. *Carbon* **1999**, *37*, 15–20. [CrossRef]
20. Suzuki, R.; Andrade, A.; Sousa, J.; Rollemberg, M. Preparation and characterization of activated carbon from rice bran. *Bioresour. Technol.* **2007**, *98*, 1985–1991. [CrossRef]
21. Namane, A.; Mekarzia, A.; Benrachedi, K.; Belhaneche-Bensemra, N.; Hellal, A. Determination of the adsorption capacity of activated carbon made from coffee grounds by chemical activation with $ZnCl_2$ and H_3PO_4. *J. Hazard. Mater. B* **2005**, *119*, 189–194. [CrossRef]
22. Bouchelkia, N.; Mouni, L.; Belkhiri, L.; Bouzaza, A.; Bollinger, J.-C.; Madani, K.; Dahmoune, F. Removal of lead(II) from water using activated carbon developed from jujube stones, a low-cost sorbent. *Sep. Sci. Technol.* **2016**, *51*, 1645–1653. [CrossRef]
23. Teng, H.; Yeh, T.; Hsu, L. Preparation of activated carbon from bituminous coal with phosphoric acid activation. *Carbon* **1998**, *36*, 1389–1395. [CrossRef]

24. Evans, M.J.B.; Halliop, E.; MacDonald, J.A.F. The production of chemically-activated carbon. *Carbon* **1999**, *37*, 269–274. [CrossRef]
25. Ubago-Perez, R.; Carrasco-Marin, F.; Fairen-Jimenez, D.; Moreno-Castilla, C. Granular and monolithic activated carbons from KOH-activation of olive stones. *Microporous Mesoporous Mater.* **2006**, *92*, 64–70. [CrossRef]
26. Carrott, P.; Carrott, M.R.; Mourao, P. Pore size control in activated carbons obtained by pyrolysis under different conditions of chemically impregnated cork. *J. Anal. Appl. Pyrolysis* **2006**, *75*, 120–127. [CrossRef]
27. Hu, Z.; Vansant, E. Synthesis and characterization of a controlled-micropore-size carbonaceous adsorbent produced from walnut shell. *Microporous Mater.* **1995**, *3*, 603–612. [CrossRef]
28. Lillo-Rodenas, M.; Marco-Lozar, J.; Cazorla-Amoros, D.; Linares-Solano, A. Activated carbons prepared by pyrolysis of mixture of carbon precursor alkaline/hydroxide. *J. Anal. Appl. Pyrolysis* **2007**, *80*, 166–174. [CrossRef]
29. Shi, C.; Chen, Y.; Yu, Z.; Li, S.; Chan, H.; Sun, S.; Chen, G.; He, M.; Tian, J. Sustainable and superhydrophobic spent coffee ground-derived holocellulose nanofibers foam for continuous oil/water separation. *Sustain. Mater. Technol.* **2021**, *28*, e00277. [CrossRef]
30. Jutakridsada, P.; Prajaksud, C.; Kuboonya-Aruk, L.; Theerakulpisut, S.; Kamwilaisak, K. Adsorption characteristics of activated carbon prepared from spent ground coffee. *Clean Technol. Environ. Policy* **2016**, *18*, 639–645. [CrossRef]
31. Langmuir, I. The adsorption of gases on plane surfaces of glass, mica and platinum. *J. Am. Chem. Soc.* **1918**, *40*, 1361–1402. [CrossRef]
32. Freundlich, H.M.F. Over the adsorption in solution. *J. Phys. Chem.* **1906**, *57*, 385–471.
33. Butler, J.; Ockrent, C. The surface tensions of solutions containing two surface-active solutes. *J. Phys. Chem.* **1930**, *34*, 2841–2859. [CrossRef]
34. Temkin, M.; Pyzhev, V. Kinetics of ammonia synthesis on promoted iron catalyst. *Acta Phys. Chem. USSR* **1940**, *12*, 327–357.
35. Dubinin, M.; Radushkevich, L. The equation of characteristic curve of the activated charcoal. *Dokl. Akad. Nauk. SSSR* **1947**, *55*, 331–337.
36. Baghdadi, M.; Ghaffari, E.; Aminzadeh, B. Removal of carbamazepine from municipal wastewater effluent using optimally synthesized magnetic activated carbon: Adsorption and sedimentation kinetic studies. *J. Environ. Chem. Eng.* **2016**, *4*, 3309–3321. [CrossRef]
37. Cazetta, A.; Vargas, A.; Nogami, E.; Kunita, M.; Guilherme, M.; Martins, A.; Silva, T.; Moraes, J.; Almeida, V. NaOH-activated carbon of high surface area produced from coconut shell: Kinetics and equilibrium studies from the methylene blue adsorption. *Chem. Eng. J.* **2011**, *174*, 117–125. [CrossRef]
38. Foo, K.; Hameed, B. Utilization of rice husk as a feedstock for preparation of activated carbon by microwave induced KOH and K_2CO_3 activation. *Bioresour. Technol.* **2011**, *102*, 9814–9817. [CrossRef]
39. Nitayaphat, W.; Jintakosol, J.; Engkaseth, K.; Wanrakakit, Y. Removal of Methylene Blue from Aqueous Solution by Coffee Residues. *Chiang Mai J. Sci.* **2015**, *42*, 407–416.
40. Hameed, B.; Ahmad, A. Batch adsorption of methylene blue from aqueous solution by garlic peel, an agriculture waste biomass. *J. Hazard. Mater.* **2009**, *164*, 870–875. [CrossRef]
41. Kavitha, D. Namasivayam, Experimental and kinetic studies on methylene blue adsorption by coir pith carbon. *Bioresour. Technol.* **2007**, *98*, 14–21. [CrossRef]
42. Pavan, F.; Mazzocato, A. Removal of methylene blue dye from aqueous solutions by adsorption using yellow passion fruit peel as adsorbent. *Bioresour. Technol.* **2008**, *99*, 3162–3165. [CrossRef]
43. Dogan, M.; Abak, H.; Alkan, M. Adsorption of methylene blue onto hazelnut shell: Kinetics, mechanism and activation parameters. *J. Hazard. Mater.* **2009**, *164*, 172–181. [CrossRef]
44. Al Khateeb, L.; Almotiry, S.; Salam, M.A. Adsorption of pharmaceutical pollutants onto graphene nanoplatelets. *Chem. Eng. J.* **2014**, *248*, 191–199. [CrossRef]
45. Orfanos, A.; Manariotis, I.; Karapanagioti, H. Sorption of Methylene Blue onto Food Industry Byproducts. *Trends Green Chem.* **2017**, *3*, 7046.
46. Pavlovic, M.; Nikolic, I.; Milutinovic, M.; Dimitrijevic-Brankovic, S.; Siler-Marinkovic, S.; Antonovic, D. Plant waste materials from restaurants as the adsorbent for dyes. *Hem. Ind.* **2015**, *69*, 667–677. [CrossRef]
47. Hirata, M.; Kawasaki, N.; Nakamura, T.; Matsumoto, K.; Kabayama, M.; Tamura, T.; Tanada, S. Adsorption of Dyes onto Carbonaceous Materials Produced from Coffee Grounds by Microwave Treatment. *J. Colloid Interface Sci.* **2002**, *254*, 17–22. [CrossRef] [PubMed]
48. Reffas, A.; Bernardet, V.; David, B.; Reinert, L.; Lehocine, M.; Dubois, M.; Batisse, N.; Duclaux, L. Carbons prepared from coffee grounds by H_3PO_4 activation: Characterization and adsorption of methylene blue and Nylosan Red N-2RBL. *J. Hazard. Mater.* **2010**, *175*, 779–788. [CrossRef]
49. Royer, B.; Cardoso, N.; Lima, E.; Vaghetti, J.; Simon, N.; Calvate, T.; Veses, R.C. Application of Brazilian pine-fruit shell in natural and carbonized forms as adsorbent to removal of methylene blue from aqueous solution-kinetic and equilibrium study. *J. Hazard. Mater.* **2009**, *164*, 1213–1222. [CrossRef]
50. Yang, J.; Qiu, K. Preparation of activated carbons from walnut shells via vacuum chemical activation and their application for methylene blue removal. *Chem. Eng. J.* **2010**, *165*, 209–217. [CrossRef]
51. Tan, I.; Ahmad, A.; Hameed, B. Adsorption of basic dye using activated carbon prepared from oil palm shell: Batch and fixed bed studies. *Desalination* **2008**, *25*, 13–28. [CrossRef]
52. Ozer, C.; Imamoglu, M.; Turhan, Y.; Boysan, F. Removal of methylene blue from aqueous solution using phosphoric acid activated carbon prepared from hazelnut husks. *Toxicol. Environ. Chem.* **2012**, *94*, 1283–1293. [CrossRef]

53. Gunasekar, V.; Ponnusami, V. Kinetics, equilibrium and thermodynamic studies on adsorption of methylene blue by carbonized leaf plant powder. *J. Chem.* **2012**, *13*, 1–6. [CrossRef]
54. Malarvizhi, R.; Ho, Y. The influence of pH and the structure of the dye molecules on adsorption isotherm modeling using activated carbon. *Desalination* **2010**, *264*, 97–101. [CrossRef]
55. Nowicki, P.; Kazmierczak, J.; Pietrzak, R. Comparison of physochemical and sorption properties of activated carbons prepared by physical and chemical activation of cherry stones. *Powder Technol.* **2015**, *269*, 312–319. [CrossRef]
56. Theydan, S.; Ahmed, M. Adsorption of methylene blue onto biomass-based activated carbon by $FeCl_3$ activation: Equilibrium, kinetics, and thermodynamic studies. *J. Anal. Appl. Pyrolysis* **2012**, *97*, 116–122. [CrossRef]
57. Karagoz, S.; Tay, T.; Ucar, S.; Erdem, M. Activated carbons from waste biomass by sulfuric acid activation and their use on methylene blue adsorption. *Bioresour. Technol.* **2008**, *99*, 6214–6222. [CrossRef]